ACS OMEGA

Open Access

http://pubs.acs.org/journal/acsodf

Article

Excellent Pd-Loaded Magnetic Nanocatalyst on Multicarboxyl and Boronic Acid Biligands

Haijiao Jia, Mengqi Cheng, Ran Zhao, Pingyi Zheng, Fangfang Ren, Yaqin Nan, Mengting Huang, and Youxin Li*

Cite This: *ACS Omega* 2024, 9, 17817−17831

Read Online

ACCESS | Metrics & More | Article Recommendations | Supporting Information

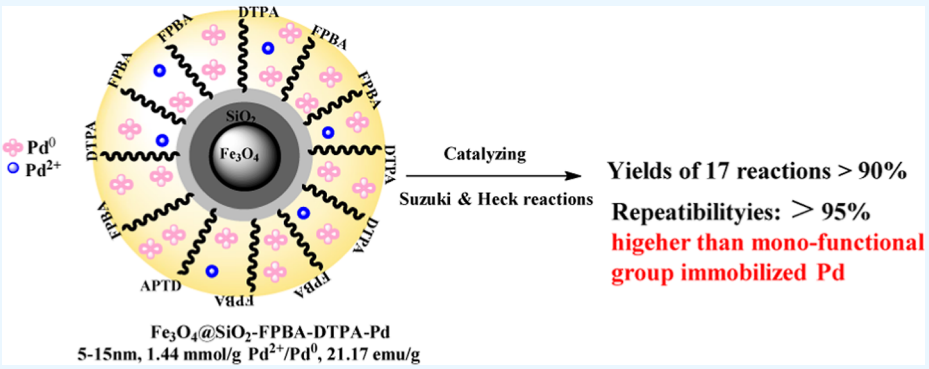

ABSTRACT: An effective palladium nanocatalyst (Fe_3O_4@SiO_2−FPBA−DTPA−Pd) was proposed and prepared, which was immobilized on magnetic silica with ethylenediamine pentaacetic acid and formylphenylboronic acid as biligands. A series of characterizations showed that Fe_3O_4@SiO_2−FPBA−DTPA−Pd was 5−15 nm and contained 1.44 mmol/g Pd^{2+}/Pd^0. It was stable below 232.7 °C, and its saturation magnetization value was 21.17 emu/g which was easily recycled by a magnet. Its catalytic ability was evaluated through 7 Suzuki reactions and 15 Heck reactions. Results showed that the yields of 14 reactions catalyzed by Fe_3O_4@SiO_2−FPBA−DTPA−Pd were more than 90%, while were better than those of the other two immobilized Pd catalysts on a single diethyltriamine pentaacetic acid (DTPA) group or boronic acid group. Moreover, Fe_3O_4@SiO_2−FPBA−DTPA−Pd showed good reusability in both Suzuki and Heck reactions. In two model Suzuki and Heck reactions, after seven cycles, its yields were still above 95% without significant loss, which exceeded those of many reported catalysts; therefore, it has great potential in future large-scale industrial production.

1. INTRODUCTION

With the development of science and industrial technology, a large number of abundant products are being produced, but the production process frequently refers to high consumption, excessive pollution, and other problems.[1] This is not in line with the sustainable and green development pursued by the current society.[2,3] Catalysts can decrease wasteful loss, energy use, and environmental contamination while accelerating reactions, improving the atomic utilization rate and reaction yield.[2−4] Therefore, catalysts have been widely studied and applied in recent years, especially the transition metal catalysts that could catalyze cross-coupling reactions in synthetic chemistry, such as Suzuki, Heck, Sonogashira, Hiyama, and Kumada reactions. Cross-coupling reactions are the main methods of C−C bond construction, which is the basic structure of organic matter. Oil, coal mines, natural gas, pharmaceuticals, conjugated polymers, and other valuable commodities are examples of organic matter that has a close relationship to humans in the process of life and production.[5−8] With the emergence of more studies and variants, Suzuki and Heck reactions show many advantages, such as mild reaction, solvent tolerance, simple operation, moderate toxicity, and high stereoselectivity.[9−14] Palladium is the most effective catalyst in these reactions due to its high activity and selectivity.[15]

The traditional homogeneous palladium catalysts (palladium acetate and palladium chloride) can be dissolved in a reaction medium, with a large degree of dispersion and high catalytic activity. High stereoselectivity can also be shown under mild conditions. But it also has many shortcomings. For example, metal palladium is difficultly separated from the reaction

Received: September 18, 2023
Revised: November 28, 2023
Accepted: March 27, 2024
Published: April 10, 2024

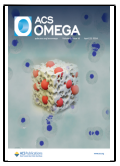

https://doi.org/10.1021/acsomega.3c07133
ACS Omega 2024, 9, 17817−17831

system, resulting in the waste of heavy metals.[16−18] In the process of large-scale industrial production, it incurs a high cost, which is not conducive to the development of enterprises. Moreover, most homogeneous Pd catalysts require ligands [phosphine,[19] dibenzyl acetone (dba),[20] and carbene[21] to enhance and prolong the activity of the catalyst. However, these ligands are expensive and even have some toxicity. They also have great limitations on environmental protection and practical production conditions. Thus, a highly active and recyclable Pd catalyst is still a major research direction.

In recent years, a variety of materials such as metal−organic frameworks (MOFs),[22] metal oxides,[23] silica,[24] resins,[25] and ionic liquids[23] were used to support Pd as catalysts. However, the aggregation and leaching of palladium[16] affect their catalytic ability. In addition, most heterogeneous catalysts require centrifugation or filtration for separation, and the operational processes are complicated.[26] As well-known to us, magnetic nanoparticles (MNPs) have a nanometer size, a large specific surface area, a high degree of dispersion, and more catalytic active sites,[15,27−29] which are the preferable materials for palladium immobilization. Moreover, the magnetically immobilized Pd catalyst is easy to magnetically separate and reuse,[30] so it has been extensively studied.

To promote the development of the immobilized Pd, some efforts were made in our laboratory. For example, a highly efficient heterogeneous catalyst (Fe_3O_4@SiO_2−APBA−Pd) was successfully synthesized.[31] It was prepared by using magnetic Fe_3O_4-coated silicon as the support, 3-aminophenylboric acid (APBA) as the modifier, and palladium acetate as the catalyst precursor. The catalyst in reusability was not satisfactory. Diethyltriamine pentaacetic acid (DTPA) could stabilize Pd,[32] but its catalytic ability was limited.

To further improve the repeatability and catalytic ability of the heterogeneous Pd catalyst, formylphenylboronic acid (FPBA) and DTPA groups were simultaneously introduced to the support material and a novel Pd nanocatalyst (Fe_3O_4@SiO_2−FPBA−DTPA−Pd) was prepared in this paper. The effect of DTPA and boronic acid (BA) group as coligands and FPBA on immobilization of palladium was investigated. The Pd-containing solutions before and after immobilization were analyzed by ultraviolet (UV) spectroscopy. The prepared Pd catalysts were characterized by Fourier transform infrared (FT-IR) spectroscopy, scanning electron microscopy (SEM), transmission electron microscopy (TEM), energy-dispersive X-ray spectroscopy (EDS), inductively coupled plasma optical emission spectroscopy (ICP-OES), X-ray photoelectron spectroscopy (XPS), vibrating sample magnetometer (VSM), and thermogravimetric analysis (TGA). In order to assess the catalytic performance and repeatability of the catalyst, a battery of Suzuki and Heck coupling reactions were performed. Products were analyzed by high-performance liquid chromatography (HPLC) and identified by nuclear magnetic resonance (NMR).

2. EXPERIMENTAL SECTION

2.1. Reagents and Chemicals. Unless otherwise stated, chemicals and reagents were used as received without further purification. Sodium cyanoborohydride (95%), formylphenylboronic acid (4-FPBA, 97%), sodium acetate (98%), potassium hydroxide (90%), and ethyl acrylate (>99.0%) were from Meryer Chemical Technology Co., Ltd. (Shanghai, China). 4-Phenylbenzonitrile (98%) was from Tianjin Heowns Biochemical Technology Co., Ltd. (Tianjin, China). Palladium acetate [$Pd(OAc)_2$, 47% Pd, 98%] was from Shanghai Eybridge Chemical Technology Co., Ltd. (Shanghai, China). *Trans*-1,2-stilbene (99.99%), 3-aminopropyl triethoxysilane (APTES, 98%), 4-bromobenzonitrile (99.73%), and 4-bromobenzaldehyde (98%) were from Shanghai Bide Pharmaceutical Technology Co., Ltd. (Shanghai, China). 4-Nitrobiphenyl (98%), *p*-biphenylcarboxaldehyde (99%), and 1-bromo-4-nitrobenzene (>99.0%) were from Aladdin Biochemical Technology Co., Ltd. (Shanghai, China). 4-Acetylbiphenyl (99%) and 4-bromoacetophenone (98%) were from 3A Chemicals Technology Co., Ltd. (Shanghai, China). Iodobenzene (99%), triethylamine (99.0%), and methyl acrylate (>99.0%) were from Macklin Biochemical Co., Ltd. (Tianjin, China). Styrene (99%) was from Rhawn Chemical Technology Co., Ltd. (Shanghai, China). Acrylic acid (99%), cinnamic acid (99%), methyl cinnamate (99%), ethyl cinnamate (99%), 4-methoxyiodobenzene (99%), 4-methyliodobenzene (99%), ethyl 4-methyl cinnamate (99%), methyl 4-methylcinnamate (>98%), 4-methoxycinnamic acid (98%), 4-nitroiodobenzene (98%), ethyl 4-nitrocinnamate (98%), 3-methoxycinnamic acid (96%), 3-methoxyiodobenzene (99%), 2-methoxyiodobenzene (98%), 2-methoxycinnamic acid (99%), and dimethyl sulfoxide-D6 (99.9% D) were from Heowns Biochem Technology Co., Ltd. (Tianjin, China). Other chemicals and reagents were from Jiangtian Chemical Technology Co., Ltd. (Tianjin, China). Ultrapure water was from Yongqingyuan Pure Water Manufacturing Center Co., Ltd. (Tianjin, China).

2.2. Instruments. A series of instruments were used to characterize the prepared Pd catalysts and their intermediates. The palladium solutions before and after immobilization were scanned in the range of 200−600 nm using a Cary 60 UV−vis spectrometer (Agilent, USA). A TENSOR 27 FT-IR spectroscope (Bruker, Germany) was used to analyze the Pd nanocatalysts and their intermediates. The particle size, dispersion, shape, fine structure, and lattice fringes of the Pd catalysts were observed by a Nanosem 430 scanning electron microscope (FEI, USA) and a JEM100CXII transmission electron microscope (JEOL, Japan). A 7404-vibrating sample magnetometer (LakeShore, USA) was used to detect the magnetic properties of Fe_3O_4@SiO_2−FPBA−DTPA−Pd and silica-coated iron oxide MNPs (Fe_3O_4@SiO_2). Elemental analysis of the catalyst was performed using a Tecnai G2 F20 energy-dispersive spectrometer (Thermo Fisher, USA). TGA was carried out with a TA 550 analyzer (Discovery, USA) under N_2 flow at a heating rate of 10 °C/min ranging from 30 to 800 °C to determine the weight loss of Fe_3O_4@SiO_2−FPBA−DTPA−Pd as a function of temperature. The binding energies of Pd catalysts were characterized by a PHI-1600 X-ray photoelectron spectroscope (Thermo Fisher, USA). The content of Pd in Fe_3O_4@SiO_2−FPBA−DTPA−Pd was determined by an ICAP7400 inductively coupled plasma optical emission spectrometer (Agilent, USA). The reaction products were analyzed using a HPLC-3000 HPLC (Chuangxintongheng, China), and the structures of the reaction products were identified by a 400 MHz Ascend 400 NMR (Bruker, Germany).

2.3. Preparation of Fe_3O_4@SiO_2−FPBA−DTPA. *2.3.1. Modification of DTPA and FPBA Biligands on Fe_3O_4@SiO_2.* Amino-modified Fe_3O_4@SiO_2 (Fe_3O_4@SiO_2−NH_2) was prepared according to the previous method in our laboratory.[31] The procedure was modified. The details were as follows. 4-FPBA (51.0 mg, 0.3275 mmol) and $NaBH_3CN$ (63.0 mg) were dissolved in 50 mL of methanol. Then, 1.5000

https://doi.org/10.1021/acsomega.3c07133
ACS Omega 2024, 9, 17817−17831

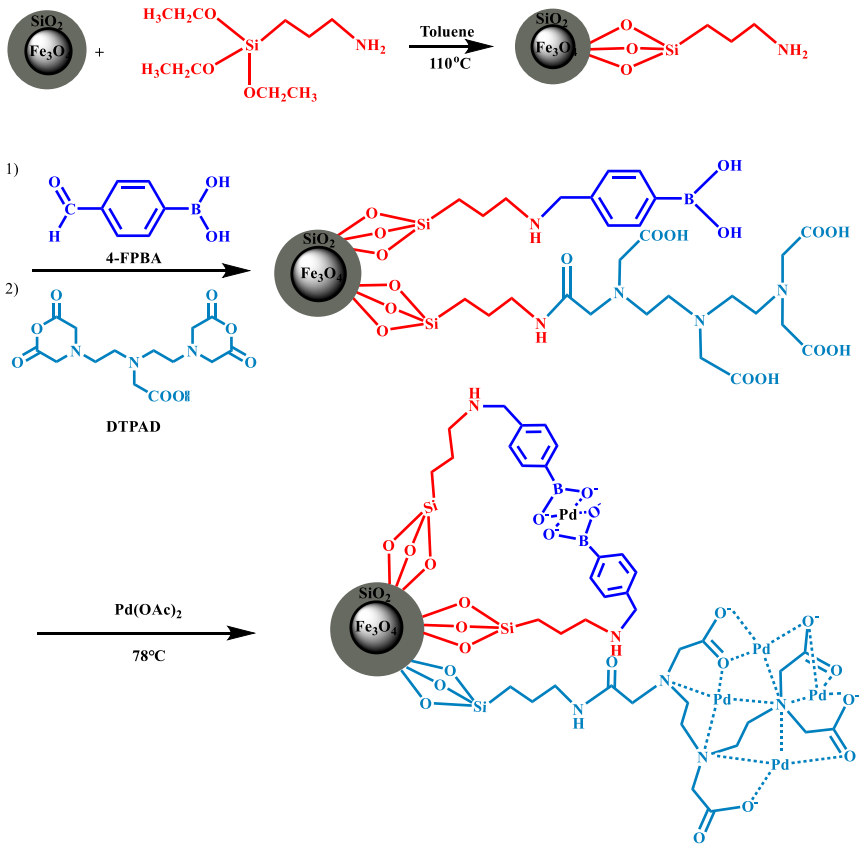

Figure 1. Preparation scheme of the Fe_3O_4@SiO_2−FPBA−DTPA−Pd catalyst.

g of Fe_3O_4@SiO_2−NH_2 was dispersed in the above solution, and the mixture was ultrasonicated for 20 min. The resulting mixture was stirred at room temperature for 24 h. The product (Fe_3O_4@SiO_2−FPBA) was collected with magnets, washed three times with methanol and water, and then dried at 60 °C for 12 h. After that, Fe_3O_4@SiO_2−FPBA was dispersed using sonication in a mixed solution of absolute alcohol (30 mL) and acetic acid (30 mL). Excess DTPA anhydride (DTPAD) was added, and the mixture was stirred at 70 °C for 12 h. The obtained MNPs were labeled as Complex I. For Complexes II and III, the amounts of 4-FPBA (0.6550 and 0.9825 mmol) and $NaBH_3CN$ (126.0 and 189.0 mg) were 2 and 3 times that of Complex I, respectively. While immobilizing Pd on single DTPA to obtain Fe_3O_4@SiO_2−DTPA, the procedure of FPBA modification was removed. Other procedures were kept the same as above.

2.3.2. Pd Immobilization. For palladium immobilization, Complex I, II, or III of 1.0000 g was added to 60 mL of anhydrous ethanol and sonicated for 20 min to keep it dispersed. Next, $Pd(OAc)_2$ (0.4582 g, 2 mmol) solution dissolved in acetonitrile was added, and the reaction was carried out for 12 h at 78 °C. Finally, the final product (called Catalyst I or Fe_3O_4@SiO_2−FPBA−DTPA−Pd) was collected and washed with copious absolute ethanol and dried for 24 h at 60 °C. Similarly, Catalyst II, Catalyst III, and Fe_3O_4@SiO_2−DTPA−Pd were immobilized on Complex II, Complex III, and Fe_3O_4@SiO_2−DTPA using the same procedure. The detailed experimental procedure is shown in Figure 1.

2.4. Suzuki Reactions. Typically, 0.5 mmol aryl halide (4-bromobenzaldehyde, 4-bromobenzonitrile, 4-bromoacetophenone, 1-bromo-4-nitrobenzene, 2-bromopyridine, 2-bromothiophene, or 4-chlorobenzaldehyde), 0.6 mmol phenylboric acid, 1.0 mmol potassium carbonate, 4 mL of ethanol−water (2:1, v/v), and 2.0 mg of Catalyst I, II, or III were added into a 25 mL three-necked flask with a cooled reflux device. Under 150 rpm mechanical stirring, the entire reaction was continued for 1 h at 60 °C. Then, the reaction product solution was filtered and fixed to 10 mL using acetonitrile and subsequently diluted as needed. Suzuki reaction products were determined by HPLC. In the reusability investigation, Suzuki reaction between 4-bromoacetophenone and phenylboric acid was employed as a model reaction. After each cycle, a magnet was used to hold the catalyst within the flask while decanting the supernatant. The catalyst was then washed with water and ethanol before being dried. Subsequently, fresh substrates were added to the flask containing the above catalyst, and the next run was started. All experiments were performed in parallel three times.

2.5. Heck Reactions. Typically, 0.50 mmol halogenated hydrocarbon, 0.75 mmol activated unsaturated hydrocarbon, 1.00 mmol triethylamine, and 3 mL of DMF were added to a 25 mL three-necked flask with a cooled reflux device. Then, 1.00 mol % Fe_3O_4@SiO_2−FPBA−DTPA−Pd was added. Under 150 rpm mechanical stirring, the reaction was carried out for 7 h at 120 °C. The reaction product solutions were filtered and fixed by acetonitrile to 10 mL and subsequently diluted as needed. Heck reaction products were measured using HPLC. In evaluating the reusability of Fe_3O_4@SiO_2−FPBA−DTPA−Pd, the unsaturated hydrocarbon was methyl acrylate, and the reaction was performed under 120 °C, 2 h, 0.50 mol % Fe_3O_4@SiO_2−FPBA−DTPA. All experiments were performed in parallel three times.

https://doi.org/10.1021/acsomega.3c07133
ACS Omega 2024, 9, 17817−17831

2.6. HPLC Conditions. The products of Suzuki and Heck reactions were analyzed by HPLC. The parameters were as follows. The column was Baulo RPS C18 column (4.6 mm × 250 mm, 5 μm) from Biomics Co. Ltd. (Tianjin, China). The temperature was room temperature. The mobile phase was a mixture of distilled water and acetonitrile (v/v, 20:80) at a flow rate of 1 mL/min. The detection wavelength was at 218 nm. All sample solutions were filtered through a 0.45 μm filter before being injected to the HPLC column, and the injection volume was 10 μL.

3. RESULTS AND DISCUSSION

3.1. Catalyst Characterization. The solutions before and after Pd immobilization were monitored by UV spectroscopy. Fe_3O_4@SiO_2−FPBA−DTPA−Pd and its intermediates were characterized by FT-IR spectroscopy, SEM, TEM, EDS, ICP-OES, XPS, VSM, and TGA.

3.1.1. Ultraviolet Spectroscopy. The residual $Pd(OAc)_2$ solution after immobilization was compared with the original $Pd(OAc)_2$ solution through UV spectra, and results are shown in Figure 2a. It was obvious that the UV spectra were quite different. The maximum absorbance of the original solution of palladium acetate was at 280 nm, which was consistent with the absorption of Pd^{2+}.[33] However, for the residual solutions after Pd immobilization, the maximum absorption peaks at 280 nm disappeared, indicating that Pd^{2+} was consumed. For the residual solution after Catalyst III preparation, a new absorption peak was observed at 251 nm, which may be attributed to the reduction of Pd^{2+} to Pd^0. For other residual solutions, the lower absorption at 280 and 251 nm indicated that more Pd was transferred to the support.

3.1.2. Fourier Transform Infrared Spectroscopy. FT-IR spectroscopy was used to characterize the chemical composition of Complex I, Complex II, Complex III, Catalyst I, Catalyst II, and Catalyst III, as well as their intermediates. Figure 2b shows the results of three magnetic supports of Complex I, Complex II, and Complex III. All MNPs had two absorption bands near 600 cm^{-1}, which were the Fe−O vibrations. The peaks at 806 and 1085 cm^{-1} corresponded to the characteristic absorption of Si−O−Si, manifesting that Fe_3O_4 granules successfully contained the SiO_2-coating layer. In the spectrum of Fe_3O_4@SiO_2−NH_2, the characteristic absorption peak at 2929 cm^{-1} and the broad peak at 3486 cm^{-1} were caused by the C−H stretching vibration of the alkyl chain and the related N−H absorption band of the amino group overlapping with the O−H stretching vibration in APTES, respectively. The characteristic absorption peak of the H−O−H bending vibration was also evident at 1641 cm^{-1}.[34] All these absorption peaks indicated that APTES was successfully bonded to the magnetic silicon sphere surface. The characteristic absorption peaks at 1741 and 1390 cm^{-1} were the C═O and C−O stretching vibrations in the carboxyl group, and the absorption band displayed at 1460 cm^{-1} corresponded to the characteristic absorption band of C−B,[35] confirming the successful bonding of DTPA and FPBA on the Fe_3O_4@SiO_2−NH_2 surface. Furthermore, the results indicated that the characteristic absorption of the three catalysts at 1738, 1454, and 1395 cm^{-1} was all weakened, which are shown in Figure 2c. These indicated that metal Pd was successfully immobilized on Complex I, Complex II, and Complex III.

3.1.3. SEM and TEM. SEM results are shown in Figure 3a−c. They revealed that the surface morphology of the three

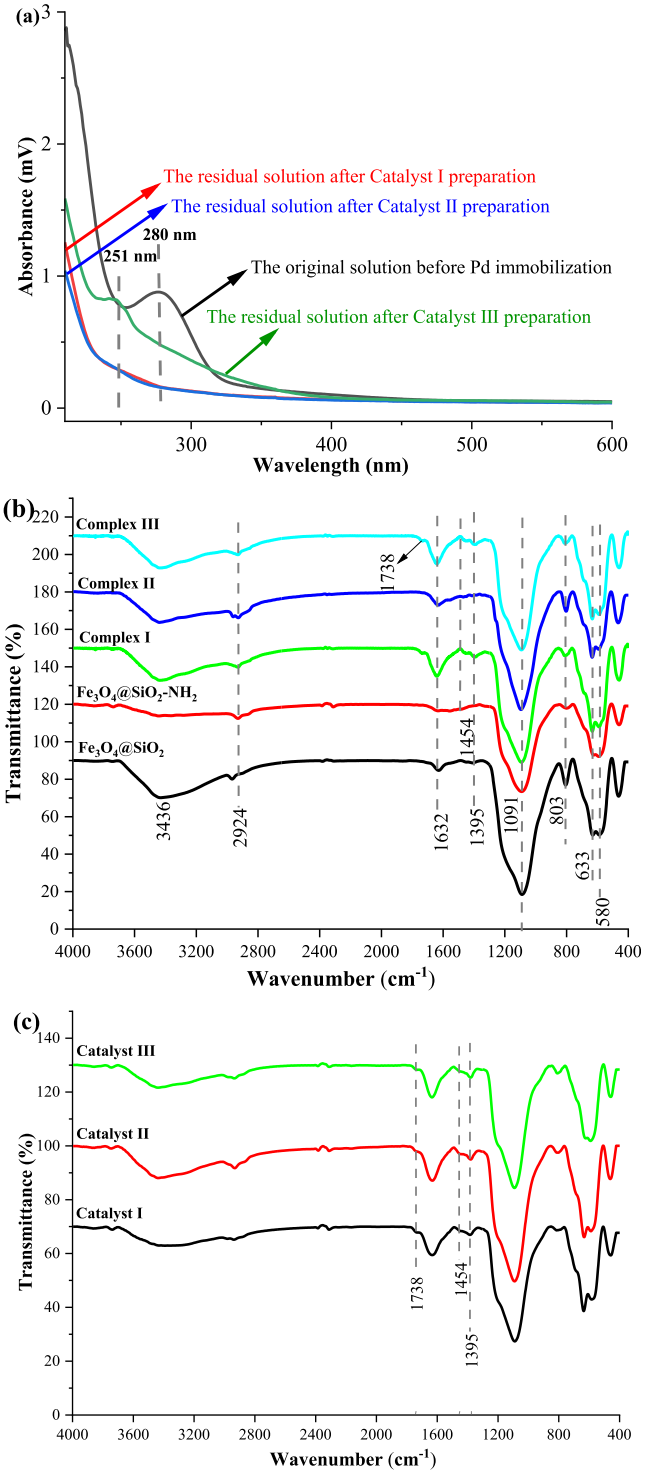

Figure 2. UV spectra of the solutions before and after palladium immobilization (a), the FT-IR spectra of Fe_3O_4@SiO_2, Fe_3O_4@SiO_2−NH_2, Complex I, Complex II, and Complex III (b), and the FT-IR spectra of Catalyst I, Catalyst II, and Catalyst III (c).

catalysts was rough. To observe the size and crystal structure of the immobilized metal palladium, three catalysts (Catalyst I, Catalyst II, and Catalyst III) were further characterized by TEM. As shown in Figure 3d−f, the three catalysts were composed of many small MNPs with diameters of about 5−15 nm. These particles were spherical. In Figure 3g−i, lattice fringes were observed in all of the high-resolution TEM images

https://doi.org/10.1021/acsomega.3c07133
ACS Omega 2024, 9, 17817−17831

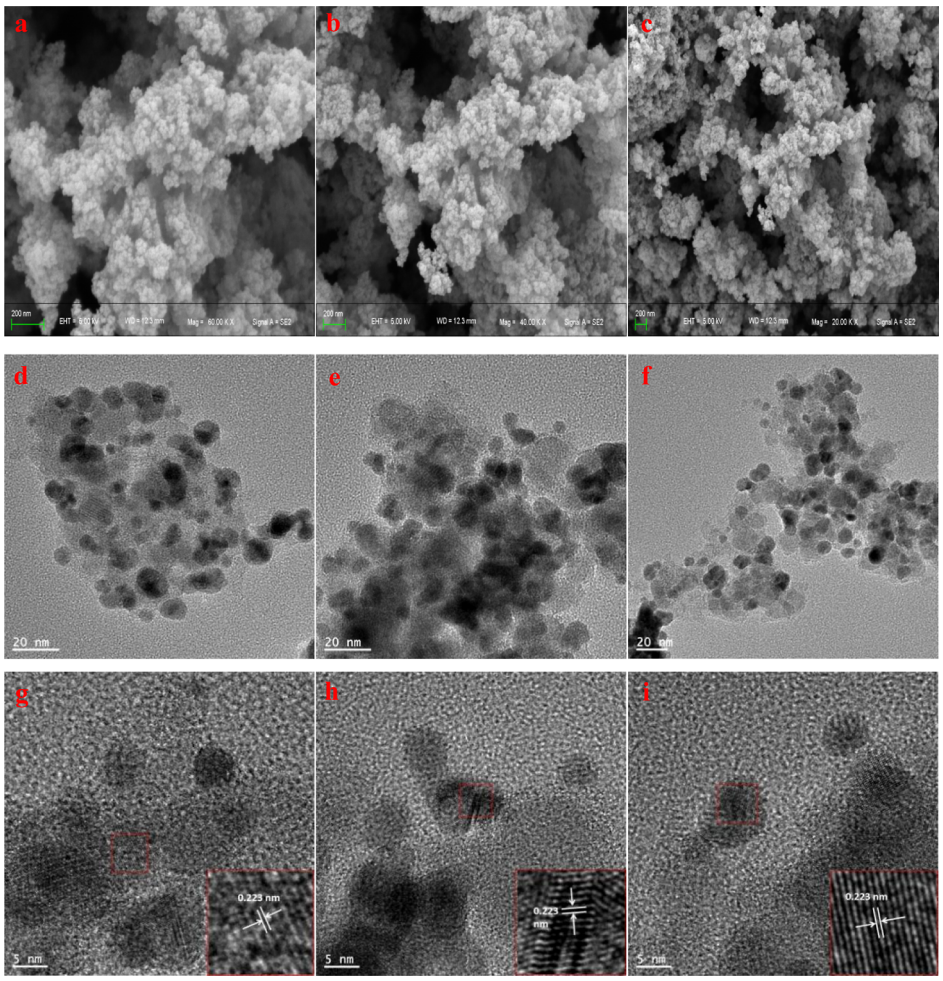

Figure 3. SEM images of Catalyst I, Catalyst II, and Catalyst III (a–c), TEM images of Catalyst I, Catalyst II, and Catalyst III (d–f), and lattice fringes of palladium atoms in Catalyst I, Catalyst II, and Catalyst III (g–i).

with a measured spacing of 0.223 nm, corresponding to the (111) crystal plane of Pd atoms.[36] These indicated that the metal palladium was successfully anchored on the surface of Complex I, Complex II, and Complex III.

3.1.4. Energy-Dispersive X-ray Spectroscopy. The elemental distribution of three biligand anchored palladium catalysts was simultaneously analyzed by EDS during TEM characterization. As shown in Figure 4, EDS spectra confirmed the presence of elements of C, N, O, Fe, Si, and Pd in the prepared Pd catalysts. In addition, EDS analysis gave the content results of each element. They were different. For Catalyst I, contents of N, O, Fe, Si, and Pd were 3.900, 56.900, 21.563, 8.237, and 9.397%, respectively. For Catalyst II, N, O, Fe, Si, and Pd were 10.880, 53.717, 18.937, 9.642, and 6.821% which contained more N and lower Pd than Catalyst I. For Catalyst III, the element contents in turns were 7.493, 59.904, 19.043, 9.392, and 4.165%, which contained the least Pd among the three catalysts.

3.1.5. X-ray Photoelectron Spectroscopy. The elements on the catalyst surface and the valence state of the active metal Pd were analyzed by XPS. The XPS full survey spectrum of Catalyst I is shown in Figure 5a. It could be seen that Catalyst I contained Fe, O, N, Pd, C, B, and Si elements, indicating the successful preparation of the Fe_3O_4@SiO_2–FPBA–DTPA–Pd catalyst. In addition, Figure 5d shows splitting peaks in the high-resolution XPS image of Pd 3d due to the spin–orbit splitting of metallic Pd. Peaks of reduced metallic Pd^0 were observed at 334.4 eV (Pd $3d_{5/2}$) and 339.7 eV (Pd $3d_{3/2}$). However, signals at 337.2 eV (Pd $3d_{5/2}$) and 342.4 eV (Pd $3d_{3/2}$) were identified as Pd^{2+}.[37] The result obtained by peak-fitting treatment showed the magnetic catalyst containing about 25.26% Pd^{2+} and 74.74% of Pd^0 which was near to 1:3 of Pd^{2+}/Pd^0. It indicated that part of Pd^{2+} was reduced to Pd^0 in the immobilization process, so the two states Pd^{2+} and Pd^0 coexisted in the Pd nanocatalyst. The reason for its reduction may be that ethanol was used as both a reaction solvent and a reducing agent in the immobilization system, thus a large amount of Pd^{2+} was reduced to Pd^0. Similarly, both Pd^0 and Pd^{2+} existed simultaneously in Catalyst II and Catalyst III, which are shown in Figure 5b,c,e,f. It was shown that the content of Pd^0 was also higher than that of Pd^{2+}.

3.1.6. Inductively Coupled Plasma Optical Emission Spectroscopy. The amounts of Pd anchored on supports were further determined by ICP-OES. Data showed that the contents of Pd in Catalysts I, II, and III were 1.44, 1.40, and 1.26 mmol/g, respectively, which were consistent with EDS results. Catalyst I had the maximum amount of Pd loading. Combining with their activity results, Catalyst I was named as Fe_3O_4@SiO_2–FPBA–DTPA–Pd and characterized in the following items.

3.1.7. Thermogravimetric Analysis. The stability of Fe_3O_4@SiO_2–FPBA–DTPA–Pd was investigated by TGA.

https://doi.org/10.1021/acsomega.3c07133
ACS Omega 2024, 9, 17817–17831

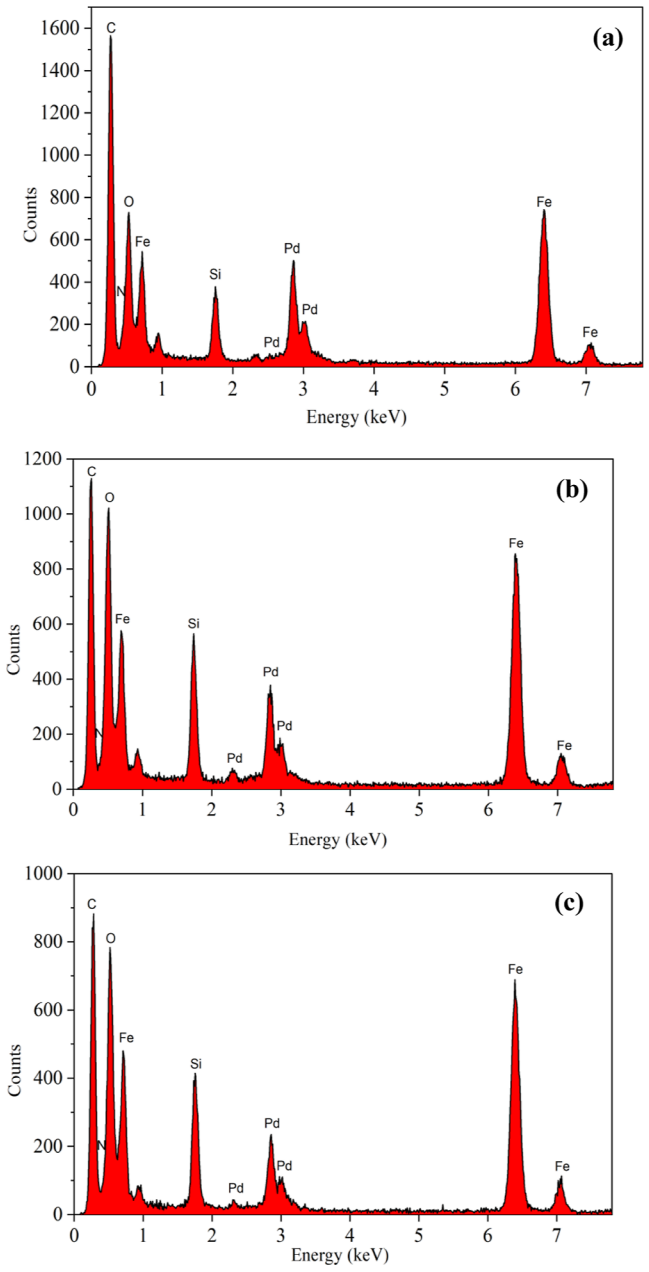

Figure 4. EDS analysis of Catalyst I (a), Catalyst II (b), and Catalyst III (c).

As shown in the TGA curve in Figure 5g, when the temperature increased from 30 to 232.7 °C, the weight of Fe_3O_4@SiO_2−FPBA−DTPA−Pd reduced to 6.41%, which was due to the loss of water through physical absorption. With temperature increasing from 232.7 to 733 °C, the weight of Fe_3O_4@SiO_2−FPBA−DTPA−Pd significantly reduced to 20.61%. The curve dropped rapidly in the range of 233−533 °C, which was the decomposition of organic matter bound to the silica surface. The latter loss was relatively slow, and it was speculated that the pore size or covalent structure of amorphous silica gel may be changed. Above 780 °C, the weight of Fe_3O_4@SiO_2−FPBA−DTPA−Pd no longer changed. Thus, Fe_3O_4@SiO_2−FPBA−DTPA−Pd was stable below 232.7 °C.

3.1.8. Vibrating Sample Magnetometer. Fe_3O_4@SiO_2−FPBA−DTPA−Pd was analyzed using VSM. The hysteresis loop curve in Figure 5h showed that the saturation magnetic intensity of Fe_3O_4@SiO_2−FPBA−DTPA−Pd was 21.17 emu/g, which was lower than that of Fe_3O_4@SiO_2 (39.87 emu/g). Undoubtedly, the presence of DTPA and FPBA on the surface of Fe_3O_4@SiO_2 caused the reduction in magnetic intensity. The magnetic response was satisfied to use an external magnet to recover the catalyst.

3.2. Evaluation of the Catalytic Ability of Fe_3O_4@SiO_2−FPBA−DTPA−Pd. *3.2.1. Suzuki Reactions.* Herein, Suzuki reaction of 4-bromoacetophenone with phenylboronic acid was employed as the model reaction. Catalyst I was chosen to catalyze the model Suzuki reaction to investigate the effect of reaction conditions on the catalytic performance. The optimal reaction solvent and base have been selected for the palladium catalyst supported by a single functional group.[31] A series of conditions were investigated including the reaction time, the dosage of the heterogeneous Pd catalyst, and the reaction temperature. Under the optimum conditions, the activities of the three catalysts were evaluated, and the products were identified by NMR (see Figures S1 and S2).

3.2.1.1. Effect of Reaction Time on the Catalytic Performance. A series of reaction times including 15, 45, 60, 90, 120, 180, and 300 min were explored at 60 °C. The data are summarized in Table 1 (entries 1−7). After 15 min, the yield of the target 4-acetyl biphenyl reached 79%, indicating a high starting reaction speed. Furthermore, with the increase of time, the yields increased. When the time reached 60 min, the yield was up 99%. The maximum yield and complete transformation of the substrate were achieved in 60 min. Therefore, 1 h was the optimal choice for the model Suzuki coupling reaction.

3.2.1.2. Effect of the Amount of Catalyst on the Catalytic Performance. Metal Pd is the active species for catalyzing the Suzuki coupling reaction; thus, the amount of heterogeneous Pd affects the catalytic efficiency. In the model Suzuki reaction, Catalyst I of 0, 2.0, 4.0, 8.0, or 16.0 mg containing 0, 2.88×10^{-3}, 5.76×10^{-3}, 11.52×10^{-3}, and 23.04×10^{-3} mmol Pd was added to study the effect of catalyst dosage on the reaction. The data can be seen in Table 1 (entries 3, 8−11). It was obvious that no reaction product appeared in the absence of the Pd catalyst. Once the Pd catalyst was added, a complete conversion could be achieved with 2 mg of Catalyst I. Upon adding 4 and 8 mg of Catalyst I, the yield of 4-acetylbiphenyl reached 100%. Therefore, a high dosage of Pd catalyst was unnecessary, and 2.0 mg of Catalyst I containing 5.76×10^{-3} mmol Pd was chosen for subsequent experiments.

3.2.1.3. Effect of Reaction Temperature on Catalytic Performance. Temperature is another important parameter that affects the Suzuki cross-coupling reaction. Thus, a series of reaction temperatures including 25, 40, 60, 80, and 90 °C were investigated. Catalyst I of 2.0 mg (5.76×10^{-3} mmol Pd) was added to a 25 mL three-neck flask containing substrates, solvent, and base. Then, the reactions were performed for 1 h at different temperatures. The results are listed in Table 1 (entries 3, 12−15). It was obvious that temperature significantly affected the activity of Catalyst I. When the temperature changed from 25 to 40 °C, the yield of 4-acetylbiphenyl gradually increased from 42 to 81%. The maximum yield was obtained at 60 °C. However, persistently elevated temperatures resulted in decreased yields. The yield was 86% at 80 °C and further decreased to 75% at 90 °C. Thus, 60 °C was selected.

https://doi.org/10.1021/acsomega.3c07133
ACS Omega 2024, 9, 17817−17831

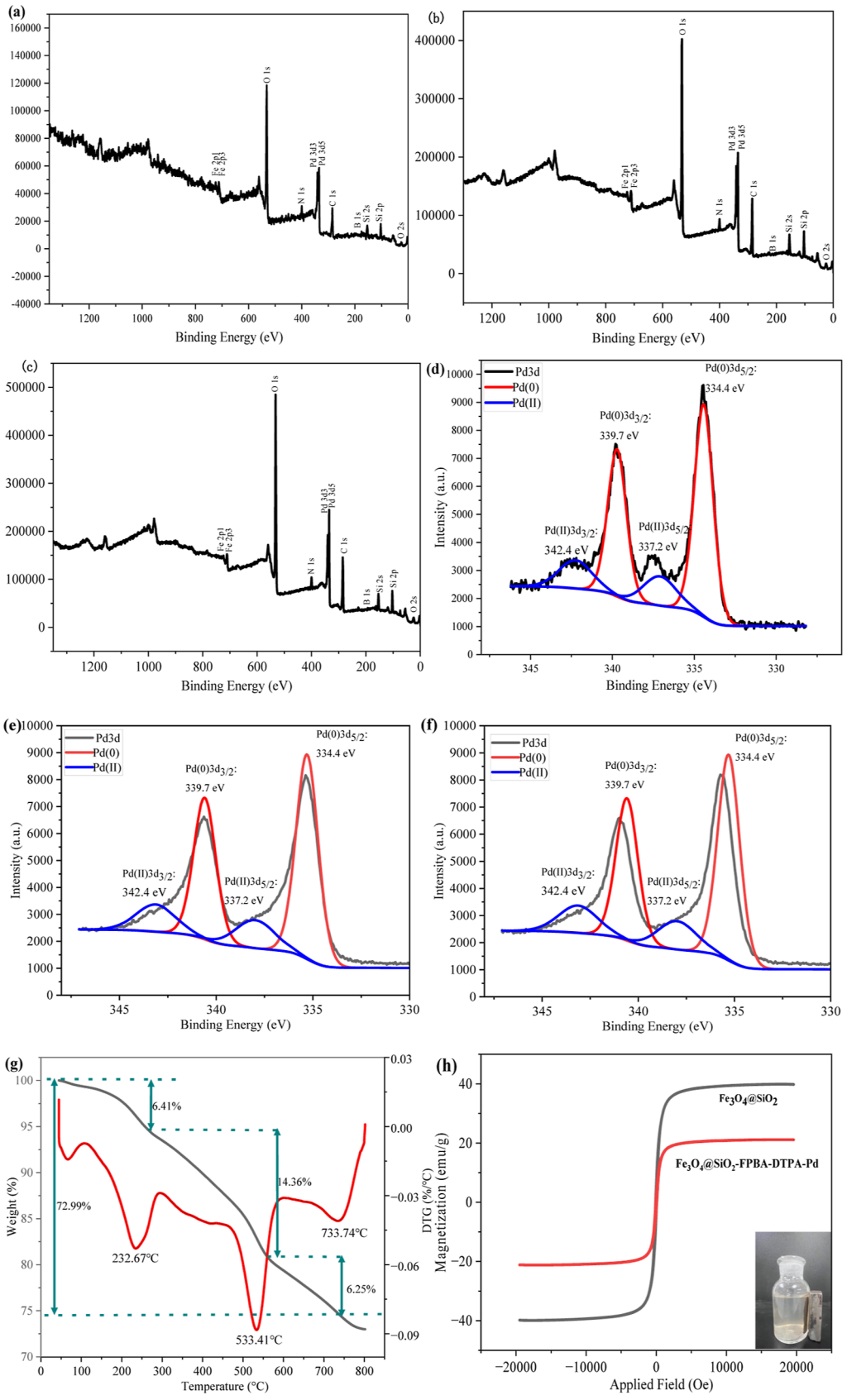

Figure 5. XPS spectra of Catalysts I, II, and III (a–c), Pd 3d scan in Catalyst I (d), Pd 3d scan in Catalyst II (e), Pd 3d scan in Catalyst III (f), TGA of Fe_3O_4@SiO_2–FPBA–DTPA–Pd (g), and VSM analysis of Fe_3O_4@SiO_2–FPBA–DTPA–Pd [(h) Photograph courtesy of Haijiao Jia. Copyright 2023].

https://doi.org/10.1021/acsomega.3c07133
ACS Omega 2024, 9, 17817−17831

Table 1. Conditions' Optimization of Suzuki Coupling Reaction between 4-Bromoacetophenone and Phenylboronic Acid[a]

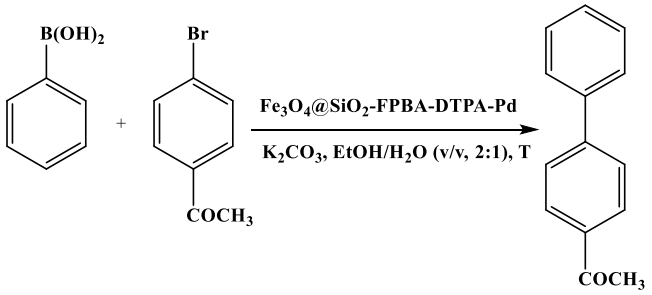

entry	time	temperature (°C)	Catalyst I (mg)	yield (%)
1	15	60	2.0	79
2	45	60	2.0	96
3	60	60	2.0	99
4	90	60	2.0	93
5	120	60	2.0	84
6	180	60	2.0	82
7	300	60	2.0	79
8	60	60	0	0
9	60	60	4.0	100
10	60	60	8.0	100
11	60	60	16.0	96
12	60	25	2.0	42
13	60	40	2.0	81
14	60	80	2.0	86
15	60	90	2.0	75

[a]Reaction conditions: 4-bromoacetophenone (0.5 mmol), phenylboronic acid (0.6 mmol), K_2CO_3 (1.0 mmol), Catalyst I, EtOH/H_2O (v/v, 2:1, 4 mL).

3.2.1.4. Evaluation of Three Supported Pd Catalysts. To investigate the cooperation effect of DTPA and BA groups as coligands for immobilizing Pd, the catalytic activity of Catalyst I, Catalyst II, and Catalyst III was evaluated via seven Suzuki reactions of different aryl halides (4-bromobenzaldehyde, 4-bromobenzonitrile, 4-bromoacetophenone 1-bromo-4-nitrobenzene, 2-bromopyridine, 2-bromothiophene, and 4-chlorobenzaldehyde) with phenylboronic acid. The catalytic products were identified by 1H NMR (see Figures S1 and S2). Table 2 shows the catalytic results of three Pd catalysts, which were compared with $Pd(OAc)_2$ and another two immobilized Pd catalysts anchored on a single DTPA group or BA group, Fe_3O_4@SiO_2−DTPA−Pd, and Fe_3O_4@SiO_2−APBA−Pd.[31] Results showed that the selectivity of the prepared Pd catalysts in seven Suzuki reactions was greater than 99%. It was also found that Catalyst I had generally good catalytic performance over Catalysts II and III, which could be attributed to the higher palladium content in Catalyst I. Moreover, the yield of Catalyst I was higher than that of Fe_3O_4@SiO_2−DTPA−Pd, Fe_3O_4@SiO_2−APBA−Pd, and $Pd(OAc)_2$. Taking the Suzuki reaction between 4-bromoacetophenone and phenylboronic acid as an example, Catalyst I obtained the high yield of 99%, which was better than $Pd(OAc)_2$ (82%), Fe_3O_4@SiO_2−DTPA−Pd (96%), and Fe_3O_4@SiO_2−APBA−Pd (64%), respectively, while Catalyst II and Catalyst III achieved 96 and 86% yields, respectively, in this reaction. Because the amount of 4-FPBA bonded to Complex I, Complex II, and Complex III increased sequentially in the catalyst preparation process, their decreased

Table 2. Performance Comparison of Fe_3O_4@SiO_2−DTPA−Pd, Catalyst I, Catalyst II, Catalyst III, and Fe_3O_4@SiO_2−APBA−Pd Catalysts in Four Suzuki Reactions[a]

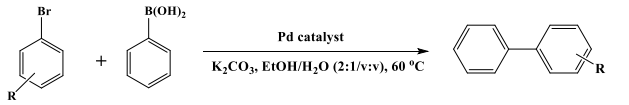

Entry	Catalyst	Substrate	Product	Yield (%)
1	Fe_3O_4@SiO_2-DTPA-Pd	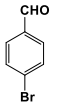	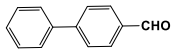	95
2	Catalyst I			98
3	Catalyst II			97
4	Catalyst III			67
5	Fe_3O_4@SiO_2-APBA-Pd			91[31]
6	$Pd(OAc)_2$			82
7	Fe_3O_4@SiO_2-DTPA-Pd	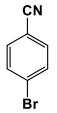	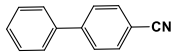	98
8	Catalyst I			98
9	Catalyst II			89
10	Catalyst III			97
11	Fe_3O_4@SiO_2-APBA-Pd			95[31]
12	$Pd(OAc)_2$			95
13	Fe_3O_4@SiO_2-DTPA-Pd	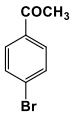	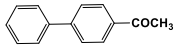	96
14	Catalyst I			99
15	Catalyst II			96
16	Catalyst III			86
17	Fe_3O_4@SiO_2-APBA-Pd			64[31]
18	$Pd(OAc)_2$			82
19	Fe_3O_4@SiO_2-DTPA-Pd	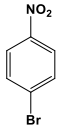	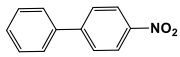	89
20	Catalyst I			93
21	Catalyst II			85
22	Catalyst III			85
23	Fe_3O_4@SiO_2-APBA-Pd			87[31]
24	$Pd(OAc)_2$			86
25	Fe_3O_4@SiO_2-DTPA-Pd		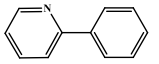	19[b]
26	Catalyst I			64[b]
27	Catalyst II			7[b]
28	Catalyst III			6[b]
29	$Pd(OAc)_2$			18[b]
30	Fe_3O_4@SiO_2-DTPA-Pd		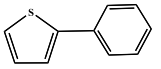	10
31	Catalyst I			5
32	Catalyst II			7
32	Catalyst III			6
34	$Pd(OAc)_2$			7
35	Fe_3O_4@SiO_2-DTPA-Pd	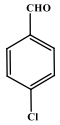	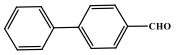	5
36	Catalyst I			10
37	Catalyst II			0
38	Catalyst III			0
39	$Pd(OAc)_2$			5

[a]Conditions: 0.5 mmol aryl halide, 0.6 mmol PBA, 1.0 mmol K_2CO_3 as the base, 2 mg catalysts, EtOH/H_2O (v/v, 2:1, 4 mL) as the solvent, 60 °C, 1 h. [b]Reaction 6 h.

yields in this case indicated that the combination of low amount of BA with the DTPA ligand was conducive to the catalytic activity improvement. Thus, it was vital to investigate the amount of two ligands in the support material. In the heterocyclic reaction of 2-bromopyridine and 2-bromothiophene, it was observed that the catalytic effect of Catalyst I still

https://doi.org/10.1021/acsomega.3c07133
ACS Omega 2024, 9, 17817−17831

Table 3. Conditions' Optimization of the Model Heck Reaction between Iodobenzene and Styrene[a]

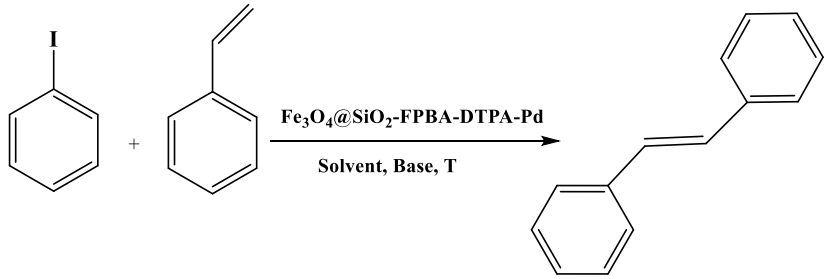

entry	solvent	base	catalyst (mol %)	yield (%)
1	ACN	Et_3N	0.34	11
2	EtOH	Et_3N	0.34	trace
3	EtOH/H_2O (v/v, 2:1)	Et_3N	0.34	trace
4	toluene	Et_3N	0.34	5
5	DMF	Et_3N	0.34	80
6	DMF/H_2O (v/v, 2:1)	Et_3N	0.34	20
7	DMF	K_2CO_3	0.34	70
8	DMF	Na_2CO_3	0.34	59
9	DMF	NaOAc	0.34	44
10	DMF	$NaHCO_3$	0.34	50
11	DMF	KOH	0.34	6
12	DMF	Et_3N	0	0
13	DMF	Et_3N	0.50	85
14	DMF	Et_3N	0.80	90
15	DMF	Et_3N	1.00	99
16	DMF	Et_3N	1.50	95

[a]Conditions: 0.5 mmol iodobenzene, 0.75 mmol styrene, 1 mmol base, 120 °C, 7 h.

exceeded that of Catalyst II, Catalyst III, and homogeneous catalyst (Table 2, entries 25−34). This phenomenon also existed in chlorine substitution reactions (Table 2, entries 35−39). Results verified that Fe_3O_4@SiO_2−FPBA−DTPA−Pd was effective in heterocyclic and chlorine substitution Suzuki reactions.

3.2.2. Heck Reactions. In Suzuki reactions, it was verified that the catalysts were different in catalytic activity under the same mass and Catalyst I showed the highest activity. Therefore, the Heck coupling reaction between iodobenzene and styrene was chosen as the model reaction, and Catalyst I (Fe_3O_4@SiO_2−FPBA−DTPA−Pd) was directly selected to investigate the effect of catalytic conditions on catalytic performance, including solvent, base, temperature, time, and the dosage of catalyst. Under the optimum conditions, the activities of the catalysts were compared, and the products were identified by NMR (see Figures S3 and S4).

3.2.2.1. Effect of Solvent on Catalyst Performance. The choice of solvent plays an important role in the activity of the catalyst. Most solvents commonly used in Heck reaction are organic reagents or mixtures of organic reagents and water. Under 120 °C as the reaction temperature, a range of solvents, including acetonitrile, ethanol, ethanol−water (v/v, 2:1), toluene, DMF, and dimethylformamide−water (v/v, 2:1), were investigated, and results are shown in Table 3 (entries 1−6). For solvents with low boiling points, like acetonitrile and ethanol, a high temperature of 120 °C resulted in solvent evaporation and low yield of the target product. DMF has both a high boiling point and a good ability to dissolve organic reactants and bases. Among all solvents selected, the maximum yield (80%) of anti-1,2-stilbenes was achieved in DMF. Therefore, DMF was chosen as the solvent for Heck reactions.

3.2.2.2. Effect of the Base on Catalyst Performance. Although the mechanism of the base is uncertain, there is no doubt that the base plays an important role in Heck reaction. Six bases, including K_2CO_3, NaOAc, Na_2CO_3, $NaHCO_3$, KOH, and Et_3N, were investigated, and results are summarized in Table 3 (entries 5, 7−11). Since the solvents and reactants in the reaction system were organic reagents, the effect of organic bases was stronger than that of inorganic bases. The best yield of anti-1,2-stilbene was 80% when triethylamine was used as the base. It was obvious that the effects of inorganic binary base were stronger than those of unary bases and strong bases. The yields of anti-1,2-stilbene were 70% for K_2CO_3, 59% for Na_2CO_3, 50% for $NaHCO_3$, 44% for NaOAc, and 6% for KOH, respectively, which were lower than that of triethylamine. Therefore, triethylamine was selected as the base in the following experiments.

3.2.2.3. Effect of Temperature and Time on Catalyst Performance. Temperature and time have a significant effect on the yield of the Heck reaction product. Thus, under the catalysis of 0.34 mol % Fe_3O_4@SiO_2−FPBA−DTPA−Pd, the effects of temperature at 100, 120, and 140 °C and time in 1, 2, 3, 4, 5, 6, 7, and 8 h on the model Heck reaction were tested. The results are summarized in Figure 6a. It could be found that the reaction rate was the fastest at the beginning of 2 h at 140 °C. With the extension of time, at 3 h, the yield of anti-1,2-stilbene at 120 °C exceeded 140 °C, reaching 63%. In the time curves at the three temperatures, a plateau was observed at 7 h, and the reaction yield did not continue to increase. When the temperature was 120 °C, the yield of anti-1,2-stilbene (80%) was higher than that of 100 °C (60%) and 140 °C (70%). Therefore, the temperature and time selected in the Heck

https://doi.org/10.1021/acsomega.3c07133
ACS Omega 2024, 9, 17817−17831

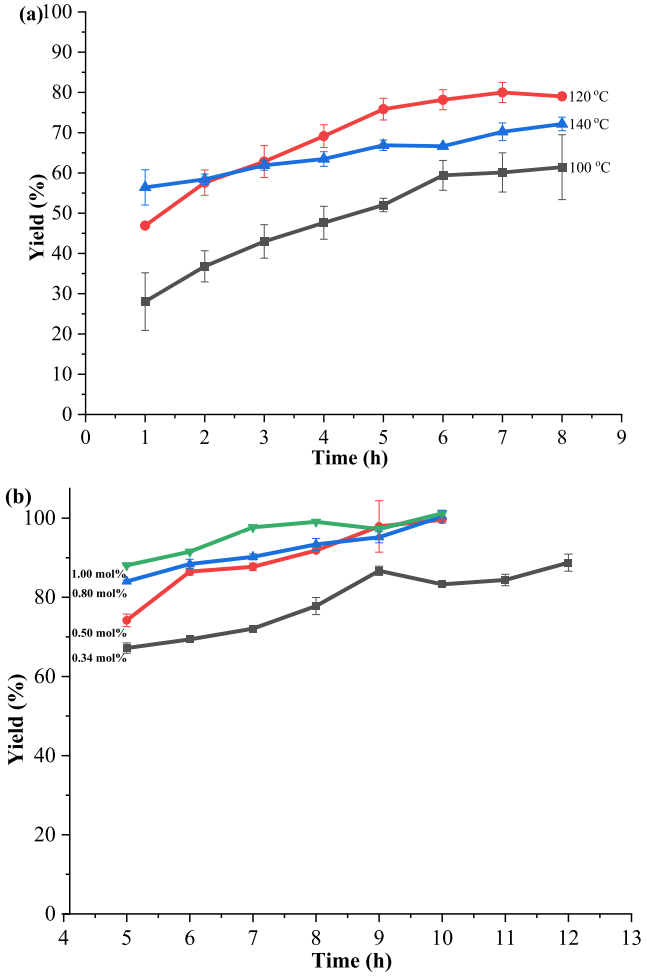

Figure 6. Effect of the time and temperature on the Heck reaction yield of iodobenzene and styrene under 0.34 mol % Fe_3O_4@SiO_2−FPBA−DTPA−Pd (a) and effect of catalyst dosage and time on the Heck reaction yield of iodobenzene and styrene (b).

coupling reaction with iodobenzene and styrene were 120 °C and 7 h, respectively.

3.2.2.4. Effect of Catalyst Dosage on Catalytic Performance. The amount of catalyst is another important parameter for the Heck reaction. The effect of a series of catalyst dosages (0, 0.34, 0.50, 0.80, 1.0, and 1.5 mol %) was studied at 120 °C for 7 h in the model Heck coupling reaction. Results are shown in Table 3 (entries 5, 12−16). It was obvious that the model Heck reaction did not occur without the Pd catalyst. With the addition of a small amount of catalyst (0.34 and 0.5 mol %), the reaction started, and the yields of *trans*-1,2-stilbenes were 80 and 85%, respectively. When the dosage of the catalyst increased to 1.0 mol %, the yield of *trans*-1,2-stilbene was up to 99%. With the continuous increase in dosage, the yield slightly decreased (95%). This indicated that more catalysts could not further improve the yield. Under the same conditions, the homogeneous catalyst palladium acetate was used and a dose of 2.00 mol % was sufficient to achieve the full conversion. Compared with the experimental conditions [5.00 mol % Pd(II) Schiff base complex 5a, 140 °C, DMF, $NaHCO_3$, argon atmosphere] of Raj Meena et al.,[38] their conditions were much more difficult to achieve the desired yield than the Fe_3O_4@SiO_2−FPBA−DTPA−Pd catalyst.

3.2.2.5. Effect of Reaction Time on Catalytic Performance. The effect of reaction time on the catalytic efficiency was further explored under a series of catalyst dosages (0.34, 0.50, 0.80, and 1.00 mol %). It could be seen from Figure 6b that the higher the dose of catalyst, the faster the rate of initiation. At the same time, it was obvious that the amount of catalyst or the extension of time increased, the yield of *trans*-1,2-stilbene increased. When the dosage of the catalyst was 0.34 mol % and the reaction time was extended to 9 h, the yield of *trans*-1,2-stilbene could reach 87%. After 12 h, the yield slightly increased (89%). As the catalyst dosage increased in the range of 0.50−1.00 mol %, the time for all of reactants to be converted to the target product decreased accordingly. At the dosage of 0.50 mol % Fe_3O_4@SiO_2−FPBA−DTPA−Pd, the yield of 92% could be achieved in 8 h. After 10 h, the yield could rise to 100%. For 0.80 mol % Fe_3O_4@SiO_2−FPBA−DTPA−Pd, 93% of *trans*-1,2-stilbene was obtained in 8 h and the maximum yields were 100% in 10 h. When the amount of catalyst was 1.00 mol %, it took 8 h to obtain the maximum yield (99%).

3.2.2.6. Comparison of Pd Catalysts Supported by Bifunctional Groups and a Single Functional Group. Under the optimal conditions, the dosages of 0.50 and 1.00 mol % catalyst were used, respectively, to explore the catalyst performance of Fe_3O_4@SiO_2−FPBA−DTPA−Pd and Fe_3O_4@SiO_2−DTPA−Pd. From Figure 7, it was obvious that the Pd catalyst immobilized by the bifunctional group was superior to the palladium catalyst immobilized by the single functional group. At the dosage of 0.50 mol % catalyst, the yield of *trans*-1,2-stilbene catalyzed by Fe_3O_4@SiO_2−DTPA−Pd reached 88% after 10 h, while that of the Fe_3O_4@SiO_2−FPBA−DTPA−Pd catalyst reached 100%. At the dosage of 1.0 mol % catalyst, the yield of *trans*-1,2-stilbene catalyzed by Fe_3O_4@SiO_2−DTPA−Pd reached 87% in 9 h and that of the Fe_3O_4@SiO_2−FPBA−DTPA−Pd catalyst reached 99% in 8 h. Moreover, it could be found that whatever the palladium catalyst was supported by a single functional group or bifunctional groups, the smaller the dosage of catalyst, the longer it took to achieve high yield of *trans*-1,2-stilbene.

3.2.2.7. Applications of Fe_3O_4@SiO_2−FPBA−DTPA−Pd. To investigate the synergistic effect of DTPA and BA groups as coligands on Pd immobilization, the catalytic activity of the Fe_3O_4@SiO_2−FPBA−DTPA−Pd catalyst was further evaluated by 13 additional Heck reactions of various aryl halides (iodobenzene, 4-methyliodobenzene, 4-nitroiodobenzene, 4-methoxyiodobenzene, 3-methoxyiodobenzene, and 2-methoxyiodobenzene, 4-phenyliodobenzene, 2-iodonaphthalene, 4-bromonitrobenzene, and 4-bromoanisole) with activated unsaturated hydrocarbons (acrylic acid, methyl acrylate, and ethyl acrylate). Because −COOR is stronger electron-withdrawing group than −Ph, compounds like acrylic acid are more likely to participate in reaction than styrene. After investigating the reaction conditions of iodobenzene and methyl acrylate (see Table S1), the yield of methyl cinnamate could reach 97% in 2 h, 120 °C with 0.50 mol % Fe_3O_4@SiO_2−FPBA−DTPA−Pd. Evaluation of Fe_3O_4@SiO_2−FPBA−DTPA−Pd was done under the optimal conditions. After each reaction, the target product was qualitatively analyzed by HPLC. Then, samples were purified through a C_{18} SPE column, and the target products were confirmed by NMR. The results showed that each of the product peaks was the target product. Then, the external standard method was used to establish standard curves to compare the catalytic yields of Fe_3O_4@SiO_2−FPBA−

https://doi.org/10.1021/acsomega.3c07133
ACS Omega 2024, 9, 17817−17831

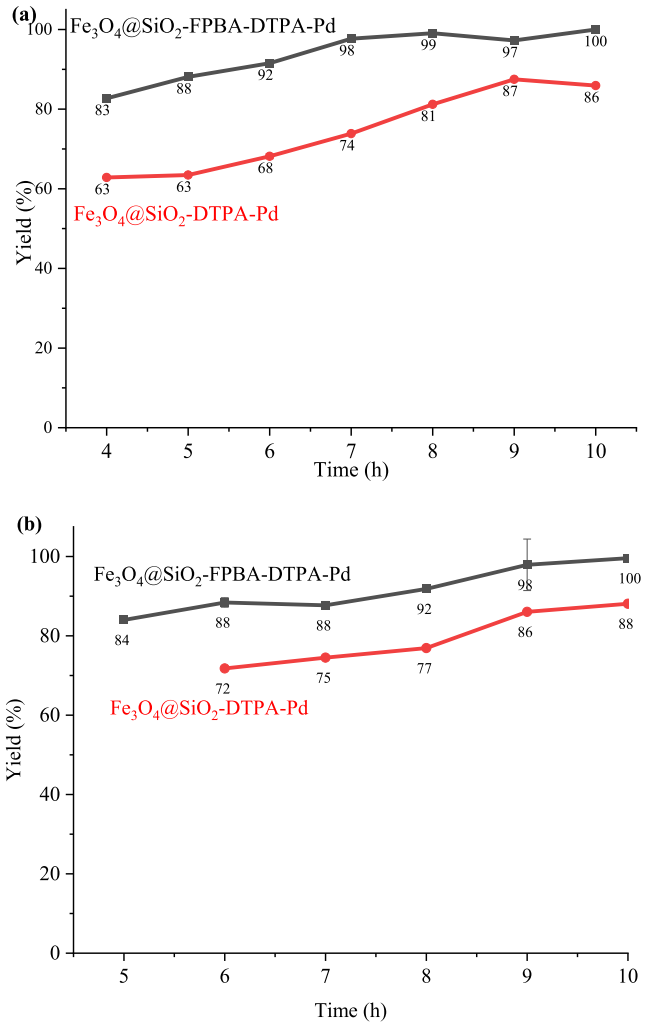

Figure 7. Comparison of the two catalysts at 0.5 mol % (a) and 1.0 mol % (b).

DTPA−Pd and Fe_3O_4@SiO_2−DTPA−Pd. The results are shown in Table 4.

First, the catalytic abilities of the two catalysts were evaluated by yields of target products. Obviously, DTPA and BA had a synergistic impact on Pd immobilized, as evidenced by the fact that the catalytic yields of the Pd catalyst supported by bifunctional groups (80−100%) were much higher than those of the Pd catalyst supported by a single functional group (60−100%). Fe_3O_4@SiO_2−FPBA−DTPA−Pd had superior catalytic performance (Table 4, entries 1−13). Second, when aryl iodide with an electron-absorbing functional groups was involved into reaction, ethyl acrylate reacted with iodobenzene or *p*-nitroiodobenzene in 2 h, the latter could reach 98%, while the former yielded only 91% and required an additional 0.5 h to reach 98% (Table 4, entries 2−3). Under the same principle, iodobenzene and 4-methoxyiodobenzene reacted with acrylic acid, the yield of the former was 98% within 2.5 h, while the latter was completely converted into the target product within 0.5 h, and the reaction time was short (Table 4, entries 5−6). Therefore, when the aryl iodide contained an electron-withdrawing functional group, the C−I bond was more active and the Heck reaction easily occurred. The same phenomenon was observed under Fe_3O_4@SiO_2−DTPA−Pd as the catalyst. The effect of the substituent position in aryl iodide on the Heck reaction was also examined. The results are also shown in Table 4 (entries 6−8). The aryl iodide of 4-CH_3O was completely converted into 4-methoxycinnamic acid within 0.5 h, while the yields of 2-CH_3O and 3-CH_3O were 92 and 92% within 3 h, respectively. It was significantly lower than that of 4-CH_3O iodobenzene. Although −CH_3O was an electron-withdrawing group, it still needed a long time to participate in the reaction and increase the yield due to the steric hindrance of 2 and 3 sites. Similarly, the same phenomenon was also observed under Fe_3O_4@SiO_2−DTPA−Pd as the catalyst. When the iodinated bicyclic structure was involved in Heck reactions, it was observed that the catalytic effect of the Fe_3O_4@SiO_2−FPBA−DTPA−Pd catalyst was similar to or slightly greater than that of the Fe_3O_4@SiO_2−DTPA−Pd-immobilized catalyst (Table 4, entries 10−11). In the reaction of bromine substitution, the yield of 4-nitroethyl acrylate could reach 90% and the yield of 4-methoxycinnamic acid could reach 79% under the catalysis of Fe_3O_4@SiO_2−FPBA−DTPA−Pd, both exceeding the catalytic effect of the Fe_3O_4@SiO_2−DTPA−Pd catalyst (Table 4, entries 12 and 13). Therefore, the bifunctional group-immobilized catalyst had a better catalytic effect on the Heck coupling reaction of bromo substitution. All in all, the catalytic activity of Fe_3O_4@SiO_2−FPBA−DTPA−Pd was obviously better than that of Fe_3O_4@SiO_2−DTPA−Pd. Moreover, the selectivity of Fe_3O_4@SiO_2−FPBA−DTPA−Pd was greater than 99% in all reactions, except for the selectivity of reactions in Table 4 (entries 6−8), which were 98%.

3.3. Stability and Recyclability of the Catalyst.

Stability and recycling are important parameters to examine for heterogeneous catalysts and one of the most important issues from a practical, economic, and environmental point of view. The stability of Pd in the prepared catalyst was tested by the hot filtration experiment. The reaction between iodobenzene and methyl acrylate was used as the model reaction, and the reaction was carried out for 30 min under the optimized conditions. Then, the catalyst was removed, and the solution was continued to react for 90 min. The yields were 78% in 30 min and 79% in 30 + 90 min, which were relatively close. It indicated that the reaction was almost stopped after removing the catalyst. The 1% difference of yield is within the error range. It is normal for some activated species to finish the conversion to product after Pd removal that maybe a contribution of 1% increase or partly. It was proved that the immobilized catalyst had high stability. Under the optimal conditions, the recyclability of Fe_3O_4@SiO_2−FPBA−DTPA−Pd was investigated by the Suzuki model reaction of 4-bromoacetophenone with phenylboronic acid and the Heck model reaction of the reaction of iodobenzene with methyl acrylate. After each reaction, the catalyst was magnetically recovered and cleaned with deionized water and absolute ethanol. It was oven-dried at 60 °C and applied in the next run. According to Figure 8, it was obvious that the yield of 4-acetyl biphenyl could reach 95% using Fe_3O_4@SiO_2−FPBA−DTPA−Pd as the catalyst which was used in the seventh run. Fe_3O_4@SiO_2−FPBA−DTPA−Pd still maintained high catalytic performance during the repetitive process. However, in the seventh reuse, the yields of Fe_3O_4@SiO_2−DTPA−Pd and Fe_3O_4@SiO_2−APBA−Pd catalysts were 92 and 91%,[31] respectively. Similar to the Heck coupling reaction, after seven runs under the catalysis of Fe_3O_4@SiO_2−FPBA−DTPA−Pd, the yield of methyl cinnamate was still 97%. There were no Pd leakage and significant weight loss after Suzuki and Heck

https://doi.org/10.1021/acsomega.3c07133
ACS Omega 2024, 9, 17817−17831

Table 4. Comparison of the Performance of Fe_3O_4@SiO_2−DTPA−Pd and Fe_3O_4@SiO_2−FPBA−DTPA−Pd Catalysts in Heck Reactions of Different Aryl Halides and Unsaturated Hydrocarbons[a]

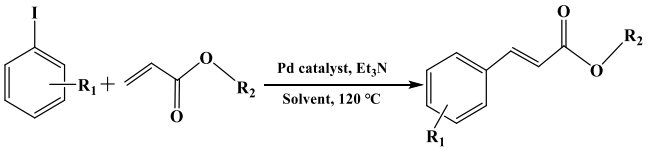

entry	R1	R2	time (h)	yield (%)		selectivity (%)
				Fe_3O_4@SiO_2−DTPA−Pd	Fe_3O_4@SiO_2−FPBA−DTPA−Pd	
1	4-CH_3	−CH_3	2.0	87	92	99
			2.5	93	99	
2	4-H	−CH_2CH_3	2.0	82	91	99
			2.5	87	98	
3	4-NO_2	−CH_2CH_3	2.0	94	98	99
4	4-CH_3	−CH_2CH_3	2.0	82	87	99
			2.5	85	98	
5	4-H	−H	2.5	80	98	99
6	4-CH_3O	−H	0.5	99	100	98
7	3-CH_3O	−H	2.0	62	80	98
			3.0	76	92	
8	2-CH_3O	−H	3.0	85	92	98
9	4-H	−CH_3	2.0	90	97	99
10	1-iodonaphthalene	−H	5.0	92	92	99
11	4-Ph	−H	2.0	77	79	99
12[b]	Br 4-NO_2	−CH_2CH_3	7.0	70	90	99
13[b]	Br 4-OCH_3	−H	7.0	65	79	99

[a]Conditions: 0.5 mmol halogenated hydrocarbon, 0.75 mmol activated unsaturated hydrocarbon, 0.50 mol % catalyst, 1.0 mmol triethylamine as the base, and 3 mL of DMF as the solvent, 120 °C. [b]Heck reaction of bromohalogenated hydrocarbons.

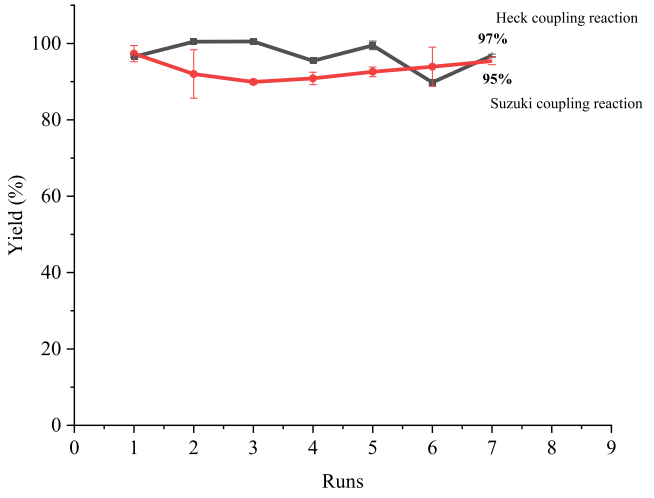

Figure 8. Reusability of the Fe_3O_4@SiO_2−DTPA−FPBA−Pd catalyst in the Heck reaction of iodobenzene and methyl acrylate and Suzuki reaction of 4-bromoacetophenone and phenylboric acid.

reactions. It could be speculated that the palladium catalyst immobilized with dual functional groups had a little loss during repeated use, and the synergistic effect of DTPA and BA on stabilizing Pd was better than that of the DTPA or FPBA single functional group.

The catalytic activity of Fe_3O_4@SiO_2−DTPA−FPBA−Pd and other supported palladium catalysts in catalyzing the Suzuki reaction of phenylboronic acid and 4-bromoacetophenone was analyzed. Results are summarized in Table 5. Some reported catalysts were very excellent, especially in the catalytic rate. However, they had apparent drawbacks. For example, the former four kinds of heterogeneous catalysts in Table 5 could not catalyze any reaction between phenylboronic acid and chloro-substituted aromatics. Although our Fe_3O_4@SiO_2−FPBA−DTPA−Pd was not preponderant in reaction time, the catalytic ability and scope were satisfactory. For example, the reaction yields between phenylboronic acid and bromo-substituted aromatics were over 93% in our work. Corresponding to APC-750@Pd in literature,[41] the yield of 4-brominated nitrobenzene and phenylboronic acid was only 85%. In addition, Fe_3O_4@SiO_2−FPBA−DTPA−Pd could catalyze the reaction of phenylboronic acid and chloro-substituted aromatics (such as chlorobenzaldehyde), and the yield of 4-biphenylcarboxaldehyde could be 10%. From these comparisons, it was obvious that Fe_3O_4@SiO_2−FPBA−DTPA−Pd was also an excellent catalyst.

Compared with other palladium-immobilized catalysts of Heck reaction (see Table 6),[43−49] the Fe_3O_4@SiO_2−FPBA−DTPA−Pd catalyst prepared in this experiment has high activity and good repeatability, is simple, and can be easily prepared. In addition, turnover number (TON) and turnover frequency (TOF) are also important parameters to evaluate the performance of catalysts. Thus, the TON and TOF of the Fe_3O_4@SiO_2−FPBA−DTPA−Pd as the catalyst were calculated as 5333.8 and 5225.3 h^{-1} in the model Heck reaction, respectively. It was clear that the TOF value of the Fe_3O_4@SiO_2−FPBA−DTPA−Pd catalyst was better than that of ref 46, 2043 h^{-1}. Therefore, the Fe_3O_4@SiO_2−FPBA−DTPA−Pd

https://doi.org/10.1021/acsomega.3c07133
ACS Omega 2024, 9, 17817−17831

Table 5. Catalytic Activities' Comparison of Fe_3O_4@SiO_2−DTPA−FPBA−Pd with Other Supported Palladium Catalysts in the Reaction of Phenylboronic Acid and 4-Bromoacetophenone

entry	catalyst (mol %)	conditions	time (min)	yield (%)	reused times	refs
1	Fe_3O_4@MCM-41@NHC@Pd	i-PrOH/H_2O (1:2), rt, X = Br	1.0	100	9	39
2	Fe_3O_4@SiO_2@NHC@Pd-MNPs	i-PrOH/H_2O (1:2), 80 °C, X = Br	5	90	6	40
3	APC-750@Pd	i-PrOH/H_2O, K_2CO_3, 80 °C	7	99	4	41
4	Fe_3O_4@SBA-15@NHC@Pd	i-PrOH/H_2O (1:2), rt, X = Br	1.0	100	10	42
5	Pd(4)Py(2)HMS	DMF/H_2O, 80 °C	360	94	3	43
6	Fe_3O_4@SiO_2−FPBA−DTPA−Pd	EtOH/H_2O (v/v, 2:1, 4 mL), 60 °C	60	99	7	this work

Table 6. Catalytic Activities' Comparison of Fe_3O_4@SiO_2−DTPA−FPBA−Pd with Other Supported Palladium Catalysts in the Reaction of Iodobenzene and Methyl Acrylate

entry	catalyst (mol %)	conditions	time (h)	yield (%)	reused times	refs
1	Pd(4)Py(2)HMS (4)	DMF/H_2O, 120 °C	16	89	3	43
2	$Pd(OAc)_2$@MNP (0.5)	NEt_3, DMF, 100 °C	1.0	97	6	44
3	Pd@MOFs-3 (1.25)	CH_3COONa_2, TBAB, DMF, 80 °C	24.0	99	4	45
4	IRMOF-3-Pd (0.165)	NEt_3, DMF, 100 °C	0.5	54	4	46
5	Pd@ACPVC (0.221)	glycol, DMAc, 110 °C	5.0	74	10	47
6	Pd NPs-ILC (0.84)	NEt_3, 100 °C	2.0	91	4	48
7	Pd-DABCO-γ-Fe_2O_3 (1)	NEt_3, DMF, 100 °C	0.5	90	5	49
8	Fe_3O_4@SiO_2−FPBA−DTPA−Pd (0.5)	NEt_3, DMF, 120 °C	2.0	100	7	this work

catalyst has great potential in future large-scale industrial production and environmental protection.

4. CONCLUSIONS

A novel bifunctional ligand-supported Pd catalyst was successfully prepared, which could be recycled by an external magnet. A series of characterizations showed that its average particle size was 5−15 nm and the surfaces of all MNPs were uneven with a Pd crystal lattice of 0.223 nm. The content of Pd in Fe_3O_4@SiO_2−FPBA−DTPA−Pd was 1.44 mmol/g with Pd^{2+}/Pd^0. Its magnetic response was 21.17 emu/g, and it was stable below 232.7 °C. The catalytic abilities of Fe_3O_4@SiO_2−FPBA−DTPA−Pd were satisfactory in 7 Suzuki reactions and 15 Heck reactions, which were better than those of the Pd immobilization catalysts on the monofunctional group and many reported heterogeneous Pd. In the process of recycling, the yield was still above 95% after 7 runs, and there was no obvious loss.

■ ASSOCIATED CONTENT

Supporting Information

The Supporting Information is available free of charge at https://pubs.acs.org/doi/10.1021/acsomega.3c07133.

HPLC chromatograms, ^1H NMR spectra, and conditions optimization of the Heck reaction model (PDF)

■ AUTHOR INFORMATION

Corresponding Author

Youxin Li − *Tianjin Key Laboratory for Modern Drug Delivery and High-Efficiency, Collaborative Innovation Center of Chemical Science and Engineering, School of Pharmaceutical Science and Technology, Tianjin University, Tianjin 300072, China;* orcid.org/0000-0001-6196-8574; Email: lyx@tju.edu.cn

Authors

Haijiao Jia − *Tianjin Key Laboratory for Modern Drug Delivery and High-Efficiency, Collaborative Innovation Center of Chemical Science and Engineering, School of Pharmaceutical Science and Technology, Tianjin University, Tianjin 300072, China*

Mengqi Cheng − *Tianjin Key Laboratory for Modern Drug Delivery and High-Efficiency, Collaborative Innovation Center of Chemical Science and Engineering, School of Pharmaceutical Science and Technology, Tianjin University, Tianjin 300072, China*

Ran Zhao − *Tianjin Key Laboratory for Modern Drug Delivery and High-Efficiency, Collaborative Innovation Center of Chemical Science and Engineering, School of Pharmaceutical Science and Technology, Tianjin University, Tianjin 300072, China*

Pingyi Zheng − *Tianjin Key Laboratory for Modern Drug Delivery and High-Efficiency, Collaborative Innovation Center of Chemical Science and Engineering, School of Pharmaceutical Science and Technology, Tianjin University, Tianjin 300072, China*

Fangfang Ren − *Tianjin Key Laboratory for Modern Drug Delivery and High-Efficiency, Collaborative Innovation Center of Chemical Science and Engineering, School of Pharmaceutical Science and Technology, Tianjin University, Tianjin 300072, China*

Yaqin Nan − *Tianjin Key Laboratory for Modern Drug Delivery and High-Efficiency, Collaborative Innovation Center of Chemical Science and Engineering, School of Pharmaceutical Science and Technology, Tianjin University, Tianjin 300072, China*

Mengting Huang − *Tianjin Key Laboratory for Modern Drug Delivery and High-Efficiency, Collaborative Innovation Center of Chemical Science and Engineering, School of Pharmaceutical Science and Technology, Tianjin University, Tianjin 300072, China*

Complete contact information is available at: https://pubs.acs.org/10.1021/acsomega.3c07133

Author Contributions

Haijiao Jia conceived, designed, and performed the experiments and analyzed the data; **Fangfang Ren** performed part of Suzuki experiments and analyzed the data; **Mengqi Cheng**,

https://doi.org/10.1021/acsomega.3c07133
ACS Omega 2024, 9, 17817−17831

Ran Zhao, Yaqin Nan, Pingyi Zheng, and Mengting Huang helped to develop and validate the Suzuki and Heck reaction conditions; **Youxin Li** provided the concept of this research and managed all the experimental and writing process as the corresponding authors; and all authors discussed the results, commented on the manuscript, and agreed to the published version of the manuscript.

Notes

The authors declare no competing financial interest.

■ ACKNOWLEDGMENTS

This research was funded by the National Natural Science Foundation of China (no. 21605112). All authors gratefully acknowledge the support.

■ ABBREVIATIONS

Pd, palladium; FPBA, 4-formylphenylboronic acid; DTPA, ethylenediaminepentaacetic acid; DMF, *N*,*N*-dimethylformamide; MOFs, metal−organic frameworks; Fe_3O_4@SiO_2, silica-coated iron oxide magnetic nanoparticles; Fe_3O_4@SiO_2−FPBA−DTPA, FPBA- and DTPA-modified silica-coated magnetic Fe_3O_4 nanoparticles; Fe_3O_4@SiO_2−FPBA−DTPA−Pd, FPBA- and DTPA-modified silica-coated magnetic Fe_3O_4 nanoparticles supported palladium; Fe_3O_4@SiO_2−DTPA−Pd, DTPA-modified silica-coated magnetic Fe_3O_4 nanoparticles-supported palladium; MNPs, magnetic nanoparticles; UV, ultraviolet; FT-IR, Fourier transform infrared; SEM, scanning electron microscopy; TEM, transmission electron microscopy; EDS, energy-dispersive X-ray spectroscopy; ICP-OES, inductively coupled plasma optical emission spectroscopy; XPS, X-ray photoelectron spectroscopy; VSM, vibrating sample magnetometry; TGA, thermogravimetric analysis; NMR, nuclear magnetic resonance; HPLC, high-performance liquid chromatography

■ REFERENCES

(1) Guo, Y. Y.; Xia, X. N.; Zhang, S.; Zhang, D. P. Environmental Regulation, Government R&D Funding and Green Technology Innovation: Evidence from China Provincial Data. *Sustainability* **2018**, *10*, 940.

(2) Jum'a, L.; Zimon, D.; Ikram, M.; Madzík, P. Towards a sustainability paradigm; the nexus between lean green practices, sustainability-oriented innovation and Triple Bottom Line. *Int. J. Prod. Econ.* **2022**, *245*, 108393.

(3) Ying, S.; Guan, Z. R.; Ofoegbu, P. C.; Clubb, P.; Rico, C.; He, F.; Hong, J. Green synthesis of nanoparticles: Current developments and limitations. *Environ. Technol. Innovation* **2022**, *26*, 102336.

(4) Li, Z.; Liu, F. N.; Jiang, Y. Y.; Ni, P. J.; Zhang, C. H.; Wang, B.; Chen, C. X.; Lu, Y. Z. Single-atom Pd catalysts as oxidase mimics with maximum atom utilization for colorimetric analysis. *J. Nano Res.* **2022**, *15*, 4411−4420.

(5) Woo, H.; Lee, K.; Park, K. H. Optimized Dispersion and Stability of Hybrid Fe_3O_4/Pd Catalysts in Water for Suzuki Coupling Reactions: Impact of Organic Capping Agents. *Chemcatchem* **2014**, *6*, 1635−1640.

(6) Ghadiri, A. M.; Farhang, M.; Hassani, P.; Salek, A.; Talesh Ramezani, A.; Akbarzadeh, A. R. Recent advancements review Suzuki and Heck reactions catalyzed by metalloporphyrins. *Inorg. Chem. Commun.* **2023**, *149*, 110359.

(7) Jasim, S. A.; Ansari, M. J.; Majdi, H. S.; Opulencia, M. J. C.; Uktamov, K. F. RETRACTED: Nanomagnetic Salamo-based-Pd(0) Complex: an efficient heterogeneous catalyst for Suzuki−Miyaura and Heck cross-coupling reactions in aqueous medium. *J. Mol. Struct.* **2022**, *1261*, 132930.

(8) Nasir Baig, R. B.; Leazer, J.; Varma, R. S. Magnetically separable Fe3O4@DOPA−Pd: a heterogeneous catalyst for aqueous Heck reaction. *Clean Technol. Environ. Policy* **2015**, *17*, 2073−2077.

(9) Xu, Y. H.; Lu, J.; Loh, T. P. Direct Cross-Coupling Reaction of Simple Alkenes with Acrylates Catalyzed by Palladium Catalyst. *J. Am. Chem. Soc.* **2009**, *131*, 1372−1373.

(10) Farina, V. High-Turnover Palladium Catalysts in Cross-Coupling and Heck Chemistry: A Critical Overview. *Adv. Synth. Catal.* **2004**, *346*, 1553−1582.

(11) Mori, A.; Araki, T.; Miyauchi, Y.; Noguchi, K.; Tanaka, K. Asymmetric Synthesis of C_2-Symmetric Axially Chiral Biaryls through Rhodium-Catalyzed and Alkyne-Controlled Diastereoselective Double [2+2+2] Cycloaddition. *Eur. J. Org Chem.* **2013**, *2013*, 6774−6778.

(12) Gao, Z.; Feng, Y.; Cui, F.; Hua, Z.; Zhou, J.; Zhu, Y.; Shi, J. Pd-loaded superparamagnetic mesoporous NiFe2O4 as a highly active and magnetically separable catalyst for Suzuki and Heck reactions. *J. Mol. Catal. A: Chem.* **2011**, *336*, 51−57.

(13) Miyaura, N.; Suzuki, A. Stereoselective synthesis of arylated (E)-alkenes by the reaction of alk-1-enylboranes with aryl halides in the presence of palladium catalyst. *J. Chem. Soc., Chem. Commun.* **1979**, *19*, 866−867.

(14) Akba, O.; Durap, F.; Aydemir, M.; Baysal, A.; Gumgum, B.; Ozkar, S. Synthesis and characterizations of N,N,N′,N′-tetrakis (diphenylphosphino)ethylendiamine derivatives: Use of palladium(II) complex as pre-catalyst in Suzuki coupling and Heck reactions. *J. Organomet. Chem.* **2009**, *694*, 731−736.

(15) Rahimi, L.; Mansoori, Y.; Nuri, A.; Koohi-Zargar, B.; Esquivel, D. A new Pd(II)-supported catalyst on magnetic SBA-15 for C−C bond formation via the Heck and Hiyama cross-coupling reactions. *J. Appl. Organomet. Chem.* **2021**, *35*, No. e6078.

(16) Zhou, A.; Guo, R. M.; Zhou, J.; Dou, Y. B.; Chen, Y.; Li, J. R. Pd@ZIF-67 Derived Recyclable Pd-Based Catalysts with Hierarchical Pores for High-Performance Heck Reaction. *ACS Sustain. Chem. Eng.* **2018**, *6*, 2103−2111.

(17) Chung, J.; Kim, J.; Jang, Y.; Byun, S.; Hyeon, T.; Kim, B. M. Heck and Sonogashira cross-coupling reactions using recyclable Pd−Fe3O4 heterodimeric nanocrystal catalysts. *Tetrahedron Lett.* **2013**, *54*, 5192−5196.

(18) Garrett, C.; Prasad, K. The Art of Meeting Palladium Specifications in Active Pharmaceutical Ingredients Produced by Pd-Catalyzed Reactions. *Adv. Synth. Catal.* **2004**, *346*, 889−900.

(19) Fleckenstein, C. A.; Plenio, H. Sterically demanding trialkylphosphines for palladium-catalyzed cross coupling reactions—alternatives to PtBu3. *Chem. Soc. Rev.* **2010**, *39*, 694−711.

(20) Amatore, C.; Jutand, A. Role of dba in the reactivity of palladium(0) complexes generated in situ from mixtures of Pd(dba)2 and phosphines. *Coord. Chem. Rev.* **1998**, *178*−*180*, 511−528.

(21) Ha, N. V.; Dat, D. T.; Nguyet, T. T. Stereoelectronic Properties of 1,2,4-Triazole-Derived N-heterocyclic Carbenes - A Theoretical Study. *VNU J. Sci.* **2019**, *35*, 55−62.

(22) Shen, K.; Chen, L.; Long, J. L.; Zhong, W.; Li, Y. W. MOFs-Templated Co@Pd Core−Shell NPs Embedded in N-Doped Carbon Matrix with Superior Hydrogenation Activities. *ACS Catal.* **2015**, *5*, 5264−5271.

(23) Liu, W. D.; Wang, D. F.; Duan, Y. J.; Zhang, Y. H.; Bian, F. L. Palladium supported on poly (ionic liquid) entrapped magnetic nanoparticles as a highly efficient and reusable catalyst for the solvent-free Heck reaction. *Tetrahedron Lett.* **2015**, *56*, 1784−1789.

(24) Shimizu, K. I.; Koizumi, S.; Hatamachi, T.; Yoshida, H.; Komai, S.; Kodama, T.; Kitayama, Y. Structural investigations of functionalized mesoporous silica-supported palladium catalyst for Heck and Suzuki coupling reactions. *J. Catal.* **2004**, *228*, 141−151.

(25) Bakherad, M.; Jajarmi, S. A dithizone-functionalized polystyrene resin-supported Pd(II) complex as an effective catalyst for Suzuki, Heck, and copper-free Sonogashira reactions under aerobic conditions in water. *J. Mol. Catal. A: Chem.* **2013**, *370*, 152−159.

https://doi.org/10.1021/acsomega.3c07133
ACS Omega 2024, 9, 17817−17831

(26) Zhao, M.; Ou, S.; Wu, C. D. Porous Metal−Organic Frameworks for Heterogeneous Biomimetic Catalysis. *Acc. Chem. Res.* **2014**, *47*, 1199−1207.
(27) Shylesh, S.; Schünemann, V.; Thiel, W. Magnetically Separable Nanocatalysts: Bridges between Homogeneous and Heterogeneous Catalysis. *Angew. Chem., Int. Ed.* **2010**, *49*, 3428−3459.
(28) Abu-Reziq, R.; Alper, H.; Wang, D.; Post, M. L. Metal Supported on Dendronized Magnetic Nanoparticles: Highly Selective Hydroformylation Catalysts. *J. Am. Chem. Soc.* **2006**, *128*, 5279−5282.
(29) Shylesh, S.; Schweizer, J.; Demeshko, S.; Schünemann, V.; Ernst, S.; Thiel, W. Nanoparticle Supported, Magnetically Recoverable Oxodiperoxo Molybdenum Complexes: Efficient Catalysts for Selective Epoxidation Reactions. *Adv. Synth. Catal.* **2009**, *351*, 1789−1795.
(30) Panahi, F.; Zarnaghash, N.; Khalafi-Nezhad, A. Phosphanamine-functionalized magnetic nanoparticles (PAFMNP): an efficient magnetic recyclable ligand for the Pd-catalyzed Heck reaction of chloroarenes. *New J. Chem.* **2016**, *40*, 1250−1255.
(31) Aschenaki, A.; Ren, F.; Liu, J.; Zheng, W.; Song, Q.; Jia, W.; Bao, J. J.; Li, Y. Preparation of a magnetic and recyclable superparamagnetic silica support with a boronic acid group for immobilizing Pd catalysts and its applications in Suzuki reactions. *RSC Adv.* **2021**, *11*, 33692−33702.
(32) Ren, F. F.; Li, S. M.; Zheng, W. Q.; Song, Q. Y.; Jia, W. H.; Nan, Y. Q.; Jia, H. J.; Liu, J.; Bao, J. J.; Li, Y. Preparation of a novel heterogeneous palladium nanocatalyst based on carboxyl modified magnetic nanoparticles and its applications in Suzuki-Miyaura coupling reactions. *Colloids Surf., A* **2022**, *642*, 128611.
(33) Shao, M.; Li, S. L.; Jin, C.; Chen, M. H.; Huang, Z. J. Recovery of Pd(II) from Hydrochloric Acid Medium by Solvent Extraction−Direct Electrodeposition Using Hydrophilic/Hydrophobic ILs. *ACS Omega* **2020**, *5*, 27188−27196.
(34) da Silva, P. A. B.; De Souza, G. C. S.; Leotério, D. M. S.; Belian, M. F.; Silva, W. E.; Paim, A. P. S.; Lavorante, A. F. Synthesis and characterization of functionalized silica with 3,6-ditia-1,8-octanediol for the preconcentration and determination of lead in milk employing multicommuted flow system coupled to FAAS. *J. Food Compos. Anal.* **2015**, *40*, 177−184.
(35) Li, F. K.; Wang, M.; Zhou, J.; Yang, M. R.; Wang, T. T. Multifunctional boronic acid-functionalized magnetic nanohybrid: An efficient and selective adsorbent of cis-diol-flavonoids. *J. Solid State Chem.* **2021**, *302*, 122384.
(36) Fan, Q.; He, S.; Hao, L.; Liu, X.; Zhu, Y.; Xu, S.; Zhang, F. Photodeposited Pd Nanoparticles with Disordered Structure for Phenylacetylene Semihydrogenation. *Sci. Rep.* **2017**, *7*, 42172.
(37) Hajipour, A. R.; Kalantari Tarrari, M.; Jajarmi, S. Synthesis and characterization of 4-AMTT-Pd(II) complex over Fe_3O_4@SiO_2 as supported nanocatalyst for Suzuki-Miyaura and Mizoroki-heck cross-coupling reactions in water. *Appl. Organomet. Chem.* **2018**, *32*, No. e4171.
(38) Raj Meena, D.; Deepa; Jubair Aalam, M.; Chaudhary, P.; Devi Yadav, G.; Singh, S. Synthesis and structural studies of Pd(II) complexes of bidentate Schiff bases and their catalytic activities as pre-catalysts in the Mizoroki-Heck reaction. *Polyhedron* **2022**, *222*, 115931.
(39) Akkoç, M.; Buğday, N.; Altın, S.; Yaşar, S. Magnetite@MCM-41 nanoparticles as support material for Pd-N-heterocyclic carbene complex: A magnetically separable catalyst for Suzuki−Miyaura reaction. *Appl. Organomet. Chem.* **2021**, *35*, No. e6233.
(40) Akkoç, M.; Buğday, N.; Altın, S.; Kiraz, N.; Yaşar, S.; Özdemir, I. N-heterocyclic carbene Pd(II) complex supported on Fe3O4@SiO2: Highly active, reusable and magnetically separable catalyst for Suzuki-Miyaura cross-coupling reactions in aqueous media. *J. Organomet. Chem.* **2021**, *943*, 121823.
(41) Buğday, N.; Altın, N.; Yaşar, S. Palladium nanoparticle supported on nitrogen-doped porous carbon: Investigation of structural properties and catalytic activity on Suzuki−Miyaura reactions. *Appl. Organomet. Chem.* **2021**, *35*, No. e6403.
(42) Akkoç, M.; Buğday, N.; Altın, S.; Özdemir, İ.; Yaşar, S. Highly Active Fe3O4@SBA-15@NHC-Pd Catalyst for Suzuki−Miyaura Cross-Coupling Reaction. *Catal. Lett.* **2021**, *152*, 1621−1638.
(43) Paramita Das, P.; Prabhakaran, V. C.; Nanda, S.; Sen, D.; Chowdhury, B. Palladium Impregnated Amine Co-condensed Hexagonal Mesoporous Silica: A Novel Catalyst in Tailoring Suzuki and Heck Coupling Reactions in Base Free Condition. *ChemistrySelect* **2019**, *4*, 3823−3832.
(44) Zhang, Q.; Zhao, X.; Wei, H. X.; Li, J. H.; Luo, J. Silica-coated nano-Fe3O4-supported iminopyridine palladium complex as an active, phosphine-free and magnetically separable catalyst for Heck reactions. *Appl. Organomet. Chem.* **2017**, *31*, No. e3608.
(45) Gole, B.; Sanyal, U.; Banerjee, R.; Mukherjee, P. S. High Loading of Pd Nanoparticles by Interior Functionalization of MOFs for Heterogeneous Catalysis. *J. Inorg. Chem.* **2016**, *55*, 2345−2354.
(46) Nuri, A.; Vucetic, N.; Smatt, J. H.; Mansoori, Y.; Mikkola, J. P.; Murzin, D. Y. Pd Supported IRMOF-3: Heterogeneous, Efficient and Reusable Catalyst for Heck Reaction. *Catal. Lett.* **2019**, *149*, 1941−1951.
(47) Qin, M.; Wang, Q. Q.; Du, Y. J.; Shao, L. J.; Qi, C. Z.; Tao, H. Y. Encapsulating palladium nanoparticles inside ethylenediamine functionalized and crosslinked chlorinated poly(vinyl chloride) nanofibers as an efficient and stable heterogeneous catalyst for coupling reactions. *J. Phys. Chem. Solids* **2020**, *147*, 109674.
(48) Mangaiyarkarasi, R.; Priyanga, M.; Santhiya, N.; Umadevi, S. In situ preparation of palladium nanoparticles in ionic liquid crystal microemulsion and their application in Heck reaction. *J. Mol. Liq.* **2020**, *310*, 113241.
(49) Sobhani, S.; Pakdin-Parizi, Z. Palladium-DABCO complex supported on γ-Fe2O3 magnetic nanoparticles: A new catalyst for CC bond formation via Mizoroki□Heck cross-coupling reaction. *Appl. Catal., A* **2014**, *479*, 112−120.

https://doi.org/10.1021/acsomega.3c07133
ACS Omega 2024, 9, 17817−17831